ResearchGate

See discussions, stats, and author profiles for this publication at: https://www.researchgate.net/publication/231814493

Oligoaniline-Contained Electroactive Silsesquioxane Precursor for Synthesizing Novel Siliceous Materials

ARTICLE *in* MACROMOLECULES · APRIL 2007

Impact Factor: 5.8 · DOI: 10.1021/ma0622985

CITATIONS
19

READS
37

8 AUTHORS, INCLUDING:

Yi Guo
Dow Chemical Company
10 PUBLICATIONS **576** CITATIONS
SEE PROFILE

Peter I Lelkes
Temple University
286 PUBLICATIONS **5,804** CITATIONS
SEE PROFILE

Kalle Levon
Polytechnic Institute of New York University
128 PUBLICATIONS **2,096** CITATIONS
SEE PROFILE

Yen Wei
Tsinghua University
485 PUBLICATIONS **13,170** CITATIONS
SEE PROFILE

Available from: Peter I Lelkes
Retrieved on: 26 January 2016

Oligoaniline-Contained Electroactive Silsesquioxane Precursor for Synthesizing Novel Siliceous Materials

Yi Guo,[†] Andreas Mylonakis,[†] Zongtao Zhang,[†,||] Peter I. Lelkes,*[,‡] Kalle Levon,[§] Shuxi Li,[†] Qiuwei Feng,[†] and Yen Wei*[,†,⊥]

Department of Chemistry and School of Biomedical Engineering & Engineering, Drexel University, Philadelphia, Pennsylvania 19104, Department of Chemical and Biological Sciences & Engineering, Polytechnic University, Brooklyn, New York 11201, and Department of Chemistry, Jilin University, Changchun 130023, P. R. China

Received October 4, 2006; Revised Manuscript Received January 18, 2007

ABSTRACT: As analogues of the well-known conducting polymer polyaniline, aniline oligomers have been extensively investigated because of their well-defined structure, good solubility, and electroactivity. In this study, we demonstrated for the first time the successful and high-yield synthesis of a novel electroactive organo-bridged silsesquioxane precursor, *N*,*N*′-bis(4′-(3-triethoxysilylpropyl-ureido)phenyl)-1,4-quinonediimine (TSUPQD), which covalently incorporates the emeraldine form of amine-capped aniline trimer into silica frameworks via one-step coupling reaction with triethoxysilylpropyl isocyanate (TESPIC) under a mild condition. Subsequently, detailed characteristics of the resulting silsesquioxane compound along with morphological measurement were systematically studied by using spectroscopic methods, such as Fourier-transform infrared (FTIR) spectra, mass spectra (MS), nuclear magnetic resonance (NMR) spectroscopy, and X-ray powder diffraction (XRD). In addition, its electrochemical behavior was explored by UV−vis spectra and cyclic voltammetry showing that its intrinsic electroactivity was maintained upon protonic acid doping and presented two distinct oxidative states in reversible cyclic voltammetry, similar to that of polyaniline. Furthermore, the sol−gel reactions of TSUPQD with various amounts of tetraethyl orthosilicate (TEOS) were carried out to afford new electroactive hybrid siliceous materials whose properties were also studied.

1. Introduction

Considerable interest has been shown in the general area of sol−gel chemistry in the past decades, like the MCM-41s family mesostructured silica.[1] Their intrinsic properties, such as high surface area, high pore volume, and narrow pore size distribution, make them particularly promising materials in a broad range of applications, ranging from catalysis[2] and chemical separation technology[3] to biosensors.[4] Purely periodic mesoporous silica, however, is greatly limited due to restricted surface functionality and poor mechanical property. With improved functionalities, inorganic−organic hybrid siliceous materials[5] have attracted a great deal of interest. Among those, a new class of hybrid materials designated as periodic mesoporous organosilicas (PMO) pose some of the most significant improvements since 1999.[6,7] These inorganic−organic hybrid materials integrate functionalized organic groups into a silica framework as a bridge. In applying similar surfactant-mediated self-assembly methods to conventional mesoporous silica, T-type silsesquioxane precursors with the formula $(C_2H_5O)_3SiRSi(OC_2H_5)_3$, where R represents a bridging organic group, have been commonly used. Typically the resulting PMOs have a stoichiometry of $R_{0.5}SiO_{1.5}$ for the sake of maintaining structural rigidity. The uniform distribution of organic units in the silica framework enhances the activity of the functional groups and makes PMOs more attractive in some of the applications like those mentioned above. Of great interest are also some of the unique properties of the PMOs, comprised of both inorganic−organic composites and the well-ordered mesoporous structure.[8] Furthermore, the organic bridges in PMO enhance the thermal and mechanical stability as compared to conventional MCM-41 type molecular sieves.[9]

In this context, bis-silylated precursors with their unique properties may serve as nuclei for generating nanoscale hybrid materials. Although a range of diverse PMOs have been synthesized, the organic constituents reported to date were limited to short aliphatic, aromatic groups or organometallic building units.[10] Garcia et al. recently reported the synthesis of photoresponsive porous silica by taking advantage of the silicon precursor *trans*-1,2-bis[*N*-(trimethoxysilylpropyl)pyridiumyl]-ethylene (*t*-BES),[11] which chemically grafted the strong electron acceptor viologen moieties into the silica wall framework. Ozin and co-workers prepared a bifunctional hybrid PMO containing two different organic bridges, which could combine the characteristics properties of both a "flexible" methylene and a "rigid" phenylene.[12] The resulting organosilica provide for further surface functionalization while keeping the shape, mechanical strength and thermal stability tunable. Thus, it is highly desirable to develop novel precursors with other useful functional bridges, having innate conductivity and/or electroactivity.

To the best of our knowledge, there are no published reports on the synthesis of electroactive silsesquioxane precursors in the family of siliceous materials. Polyaniline is one of the most investigated conducting polymers due to its high electric conductivity based on its unique protonic doping/dedoping properties.[13] The limited processability of polyaniline[14] makes design and chemical manipulation of its nanoscale derivatives more challenging. It may be, therefore, more beneficial to use aniline oligomers because they are flexible and useful with well-

* Corresponding authors.
[†] Department of Chemistry, Drexel University.
[‡] School of Biomedical Engineering & Engineering, Drexel University.
[§] Department of Chemical and Biological Sciences & Engineering, Polytechnic University, Brooklyn.
[||] Department of Chemistry, Jilin University.
[⊥] Telephone: (office) (215) 895-2650; (lab) -1644, -2979, and -2982. Fax: (215) 895-1265. E-mail: weiyen@drexel.edu

10.1021/ma0622985 CCC: $37.00 © 2007 American Chemical Society
Published on Web 03/16/2007

Scheme 1. Synthesis of (A) *N,N′*-Bis(4′-(3-triethoxysilylpropylureido)phenyl)-1,4-quinonenediimine (TSUPQD) and (B) Trimer-Containing Hybrid Materials through the Sol−Gel Process.

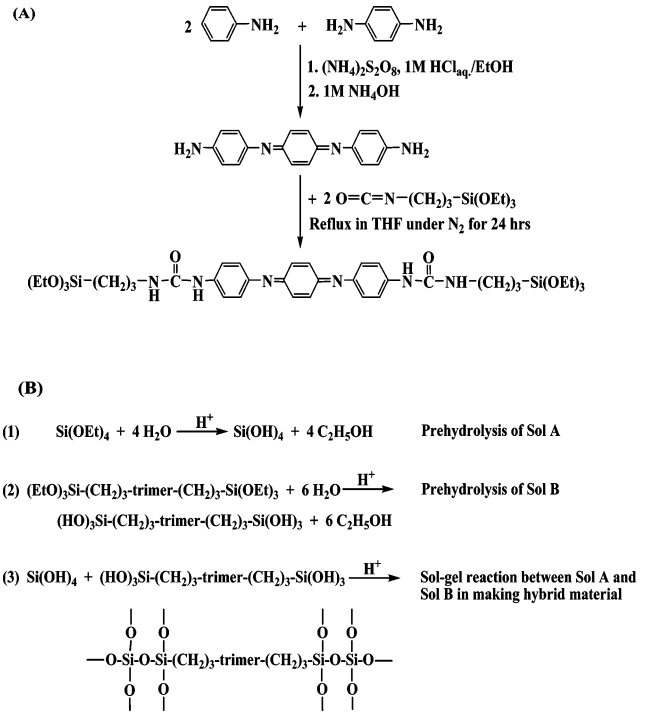

defined structure and retention of electroactivity.[15] Particularly, amine-capped aniline trimer (*N,N′*-bis(4′-aminophenyl)-1,4-quinonenediimine) is a promising substitute because this aniline trimer can exhibit electronic and optical properties which are remarkably similar to those of polyaniline.[16,17] Moreover, as an useful model for polyaniline, aniline trimer works as a useful material[18] in corrosion protection since it can form distinctive charge-transfer complexes acting as both donor and acceptor.[19]

The goal of our study is to covalently incorporate electroactive moieties into silica and other metal oxide networks. In this paper, we present the high-yield synthesis of a novel aniline trimer−siliceous precursor compound, *N,N′*-bis(4′-(3-triethoxysilylpropyl-ureido)phenyl)-1,4-quinonenediimine (TSUPQD), via a one-step coupling reaction between the amine group of the aniline trimer and the isocyanate group of the triethoxysilylpropyl isocyanante (TESPIC). Following successful synthesis, we characterized the new compound in detail using a variety of spectroscopic methods along with electrochemical and morphological analysis. Finally, the aniline trimer−siliceous precursor compound was purified by recrystallization and employed as a precursor for new electroactive organic−inorganic hybrid materials. (Scheme 1).

2. Experimental Section

2.1. Materials and Instruments. Triethoxysilylpropyl isocyanante (TESPIC), anhydrous tetrahydrofuran and *n*-hexane were purchased from Aldrich Inc., and were used without further purification while tetraethyl orthosilicate (TEOS) was distilled before use. *N,N′*-bis(4′-aminophenyl)-1,4 quinonenediimine (emeraldine aniline trimer) was prepared according to a method developed in our group[20] and purified with acetone in a Soxhlet Extractor.

^{1}H NMR and ^{13}C NMR characterization of TSUPQD in deuterated dimethyl sulfoxide (DMSO-d_6) were performed on a Varian 300 MHz NMR spectrometer with tetramethylsilane as the internal standard while ^{29}Si NMR was performed on a Bruker DRX 400 MHz instrument. IR spectra were recorded using KBr pellets with a Perkin-Elmer 1600 Fourier transform infrared spectrometer (FT−IR). UV−vis spectra were obtained using a Perkin-Elmer Lambda 35 UV−vis spectrometer. Thermal properties were studied using TA Instruments TGA Q50 and DSC Q100. Mass spectra with both low and high resolution were carried out using VG70SE using FAB with 30 kV Cs ion bombardment as the ionization technique. X-ray data were collected by fixing aliquots of the sample powder on glass slides and measured by Rigaku XRD Giegerflex D/max-11B that had a horizontal goniometer and a Cu X-ray tube running at 45 kV and 30 MA. Elemental analysis for C, H, and N was performed by Microanalysis Inc (Wilmington, DE). The obtained hybrid materials were sputter coated with Pt, and imaged with a scanning electron microscope (SEM, XL-30 Environmental SEM-FEG).

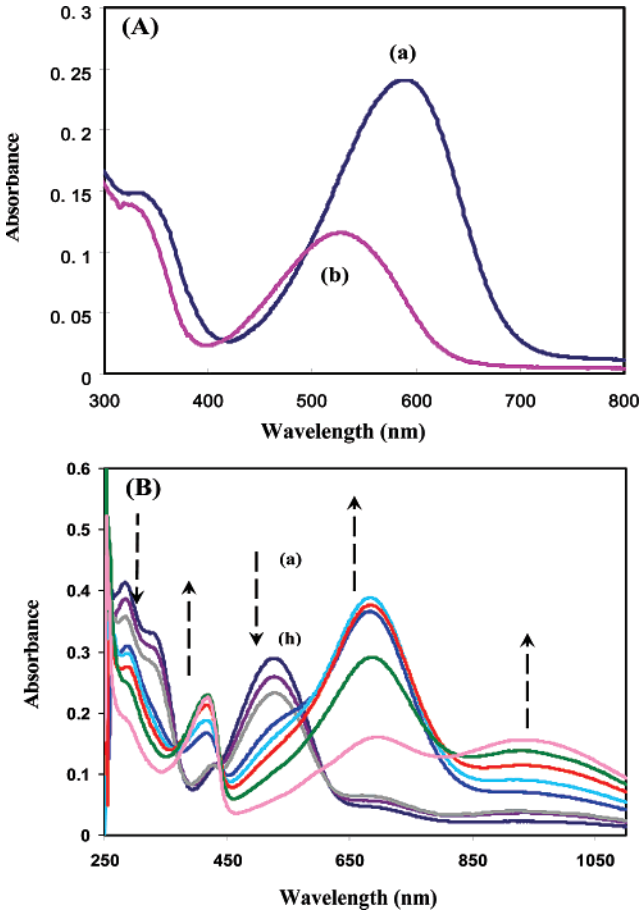

Figure 1. (A) UV−vis spectra of (a) emeraldine-base aniline trimer and (b) ethoxysilane end-capped TSUPQD. Solvent: ethanol (EtOH). Both aniline trimer and TSUPQD were purified before characterization and measured under same concentration. (B) UV−vis spectra of TSUPQD following HCl doping: (a) undoped TSUPQD, (b) doping ratio 1:1, (c) 1:10, (d) 1:200, (e) 1:500, (f) 1:1000, (g) 1:5000, and (h) 1:10000.

Electrochemical measurements were performed using an Epsilon Potensiostat interfaced to a PC computer. A three-electrode system was employed, consisting of a platinum working disk electrode (surface area (s) = 0.02 cm^2), a platinum-wire auxiliary electrode, and a reference electrode. The reference electrodes used were Ag/AgCl for aqueous solutions and Ag/Ag$^+$ (silver ions as 0.01 M $AgNO_3$ in a solution of MeCN containing 0.1 M Et_4NPF_6) for nonaqueous solutions.

2.2. Synthesis of Emeraldine Aniline Trimer: *N,N′*-Bis(4′-aminophenyl)-1,4-quinonenediimine. The aniline trimer was prepared by following the one-step approach from *N,N′*-diaminodiphenylamine developed in our group.[20] In brief, aniline monomer (10 mmol) was added and reacted in a mixture of *N,N′*-diaminodiphenylamine (5 mmol), ammonium persulfate solution (5 mmol), sodium chloride (0.15 mol), and 1 M hydrochloric acid (100 mL)

Scheme 2. Protonic Acid-Doping Structures and Mechanism for TSUPQD

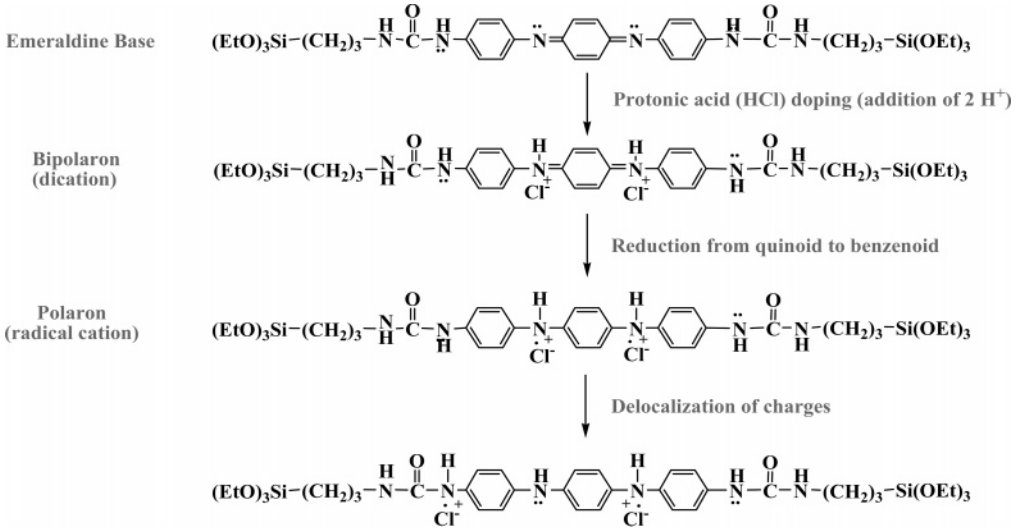

under vigorous stirring at ca. −11 °C for 2 h. After quenching with a saturated oxalic acid solution, a dark blue residue was obtained by filtering through Buchner funnel, which was washed with 1 M HCl, followed by neutralization with NH_4OH and finally dried in vacuum oven for 48 h. Subsequently, the dry product was extracted with acetone for 24 h in a Soxhlet extractor.

2.3. Synthesis of *N,N′*-Bis(4′-(3-triethoxysilylpropylureido)-phenyl)-1,4-quinonenediimine (TSUPQD). Purified aniline trimer was added dropwise into a three-neck round flask containing anhydrous THF and triethoxysilylpropyl isocyanate (TESPIC) under magnetic stirring before refluxing for 24 h under N_2 atmosphere. The molar ratio of trimer:TESPIC in the coupling reaction was 1:2.05. The small excess in the amount of TESPIC served to compensate for traces of water in the original solution. After the reaction had cooled down to room temperature, 40 mL of *n*-hexane was quickly added to the dark-red solution, and the reaction system was immediately moved into a dry ice−acetone bath for another 12 h to allow thorough precipitation. The brick-red solid was collected by filtration, washed with large amounts of *n*-hexane and dried under vacuum for 3 days at room temperature to obtain the product (TSUPQD) with a yield of ∼ 90%. Further purification was achieved by recrystallization in acetone solution. The newly formed TSUPQD was dissolved in acetone (0.01 g/mL) at its boiling point to give a saturated solution, which was subsequently filtered to remove undissolved residue and cooled at −10 °C. After 3 days, brick red rod-like crystals were obtained.

2.4. Preparation of Trimer-Containing Polymeric Hybrid Materials. The sol−gel approach developed in our group[21,22] was used to generate novel electroactive polymeric hybrid materials for the exploration of the physiochemical properties of the aniline trimer distributed within the silica framework. In general, silica sol A was first prepared by TEOS's prehydrolysis in HCl solution. Typically, 2 g (0.01 mol) of TEOS were added to a mixture of 0.48 g of 2 N HCl (aq) and 0.52 g of ethanol (anhydrous) with continuous stirring for 1 h to obtain a clear solution. In this reaction, the amount of water present was adequate for initiating the hydrolysis reaction, while HCl acted as a catalyst. Meanwhile, 2 g (2.6 mmol) of pure TSUPQD were dissolved in 100 mL of ethanol. After bath-sonication in Branson 2510 sonicator for 20 min, a homogeneous and wine-red sol B was formed. Subsequently, sol B was mixed with sol A at various weight ratios. For convenience, the electroactive aniline trimer-containing organosilica were expressed in the loading percentage of TSUPQD for the following sections. For instance, 10 wt % organosilica defines as the new hybrid material prepared by the co-condensation of 10 wt % TSUPQD and 90 wt % TEOS. The mixed sols were stirred continuously in open bottles for 12 h. After gelation in ambient conditions for 3 days and drying in a vacuum oven for 24 h, dark but transparent aniline trimer-containing hybrid materials as monoliths were obtained. As a control, the silica made from pure TEOS sol was also prepared in a similar manner. For characterization, all samples were ground into a fine powder, washed with ethanol, and dried in vacuum oven at room temperature until the final weight remained constant.

3. Results and Discussion

Section A. Structural and Physiochemical Characterization of TSUPQD. As the shortest analogue of the widely studied polyaniline, amine-capped aniline trimer has good electroactivity with three distinct oxidation states and well-defined structure.[15,19] This particular property might be very fascinating when brought into the sol−gel area. It could be a promising candidate as part of a biocompatible scaffold material for tissue engineering,[23] especially employed as electrospun nanofibrous scaffolds when fabricated with biopolymers.[24] The aniline trimer could also be used to modify electrode surfaces to increase the sensitivity and the signal/noise ratio in electrochemical applications.

3.1. UV—Vis Spectroscopic Characterization. The UV−vis spectra of the emeraldine-base aniline trimer and TSUPQD in EtOH solution are shown in Figure 1A. Similar to polyaniline, the quinoid (Q) absorption peak at ca. 520 nm and benzenoid (B) peak at ca. 330 nm are two characteristic peaks in emeraldine base (EB) form of aniline trimer, which are associated with the transition of $\pi_b-\pi_q$ from benzene unit to quinone unit and from $\pi-\pi^*$ transition in benzene unit, respectively.[25] From the absorption bands depicted in Figure 1A, the Q/B intensity ratio decreases from 1.6 to 0.84 along with a slight blue shift. This change can be caused by enhanced resonance from the formation of ureido moiety that facilitates the delocalization of electrons in benzene unit as shown in Scheme 2. As a result, the electronic concentration on quinone units can be reduced and the intensity of transition $\pi_b-\pi_q$ is thus halved. We did not observe any new absorption during the process of synthesis, indicating that the aniline trimers in the novel TSUPQD product remain in the EB form. These results suggest that the amine-capped aniline trimers are covalently grafted by TESPIC molecules with ethoxysilane end groups and there is no oxidation or transition in the oxidative state.

The emeraldine salt (ES) form of TSUPQD was generated by continuously doping the product with 2 N HCl, as evidenced by the UV−vis spectra (Figure 1B), showing dramatic changes in the absorption behavior. The concentration of the TSUPQD in the sample vials was kept constant in order to acquire the continuous evolution in the electronic spectrum. Successive

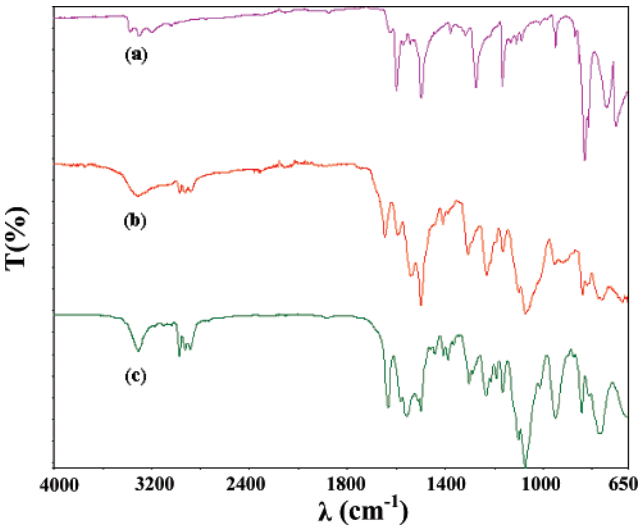

Figure 2. FTIR-spectra of (a) emeraldine-base aniline trimer, (b) freshly synthesized TSUPQD, and (c) recrystallized TSUPQD.

addition of HCl yielded remarkable changes in the electronic spectrum. The two electronic transitions respectively at about 330 and 520 nm gradually disappeared; instead, three new bands were observed at around 415, 675, and 925 nm, which are probably due to the formation of polarons (radical cations) caused by the electron transition of quinoid to benzoid units. As substitution alters quinoid peak in comparison to the amine-capped aniline trimer, the protonation bands occur at higher energy than in the trimer, which when doped with dodecylbenzenesulfonic acid (DBSA) has bands at about 425 and 800 nm.[26] Furthermore, the intensity of the new band at 675 nm accounting for the complex of trimer radical cations paired with counterions tends to decrease when reaching maximum at a molar ratio of 1:500. A possible explanation of this phenomenon is that an excess of HCl impairs the hyperfine structure and dissociates the aggregates that form the bipolaron intermediates. The result of conductivity measurement as performed conducted with a 4-probe device (PAR model 173 potentiostat/Galvanostat) is consistent with the above explanation. The HCl-doped TSUPQD at ratio of 1:500 showed a maximum conductivity of $\sim 5 \times 10^{-5}$ S/cm followed by a conductivity of $\sim 3 \times 10^{-5}$ S/cm at a ratio of 1:1000 and $\sim 1.9 \times 10^{-5}$ S/cm at a ratio of 1:200. These were significantly lower than the conductivity of the parent aniline trimer ($\sim 10^{-3}$ S/cm).

3.2. FT−IR Spectral Characterization. In the FT−IR spectra of TSUPQD in Figure 2, the shift of the broad vibrational bands from the original ca. 3400−3200 cm^{-1} to ca. 3250 cm^{-1} revealed that the aromatic amine (−NH_2) in the aniline trimer was converted into the imine (−NH) of the ureido unit (−NH−CO−NH−). The new, strong bands at ca. 2900 cm^{-1} are attributed to the presence of aliphatic sp^3 C−H stretching, while the bands at ca. 1077 cm^{-1} for C−O stretching arise from −OCH_2CH_3 group due to the substitution of the ethoxysilane units. Importantly, the presence of the carbonyl band at ca. 1680 cm^{-1} and the amide band at ca. 1560 cm^{-1} also prove the new appearance of ureido moiety. By comparison of Figure 2b and 2c, the recrystallized TSUPQD can be observed having a sharper and stronger peak for N−H stretching than the as-synthesized sample. Moreover, it is worth noting that the higher relative intensity of quinoid band at ca. 1600 cm^{-1} in Figure 2c means the impurity from as-synthesized TSUPQD was effectively removed by the recrystallization process. Meanwhile, the phenyl C−H stretching at 3020 cm^{-1}, the typical quinoid and benzenoid ring stretching at ca. 1600 cm^{-1} and 1500 cm^{-1} as well as C−N stretching at 1310 cm^{-1} and 1220 cm^{-1} are retained,[27] indicating that the characteristics of the aromatic chain in the TSUPQD are completely analogous to those of aniline trimer. Those changes are in good agreement with the structural modifications shown in Scheme 1, as the coupling reaction only occurs at the end group of aniline trimer.

3.3. ^{1}H NMR, ^{13}C NMR, and ^{29}Si NMR Spectroscopy. We further characterized TSUPQD by ^{1}H, ^{13}C, and ^{29}Si NMR spectroscopy in DMSO-d_6 with TMS as internal standard. (Supporting Information, Figure S1). All the NMR peak assignments are listed below. ^{1}H NMR: $\delta = 8.55$ (singlet for two H in −(C═O)− NH− close to aromatic ring); $\delta = 7.42$, 7.00, and 6.88 (multiplet for 12 allyl H from aniline trimer); $\delta = 6.20$ (triplet for two different urea H); $\delta = 3.75$ (multiplet for 12 ethylene H in −$SiOCH_2CH_3$−); $\delta = 3.05$ (multiplet for four ethylene H close to amine group in −CH_2CH_2NH−); $\delta = 1.48$ (multiplet for four middle ethylene H in −$CH_2CH_2CH_2$−); $\delta = 1.16$ (triplet for 18 methyl H in −$SiOCH_2CH_3$-); $\delta = 0.56$ (multiplet for four ethylene H close to silica in −CH_2-CH_2CH_2Si−). ^{13}C NMR: $\delta = 162.5$ (C═O); $\delta = 158.0$, 155.8, 144.8, 138.9, 122.8, 118.2 (aryl C); $\delta = 58.2$, 19.0 (−$SiOCH_2$-CH_3-); $\delta = 42.2$, 24.0, 11.3 (−$CH_2CH_2CH_2$−). ^{29}Si NMR: $\delta = -49.98$ (Si). Also, as shown in Figure S1A, the integral area of each characteristic peak matches the theoretical number of protons quite well, which gives additional support to our interpretation of the conformation and chemical structure of resulting TSUPQD.

3.4. Mass Spectra Characterization. Mass spectra of TSUPQD (Figure S2) were recorded using fast atom bombardment (FAB) ionization. Acetone, a volatile solvent, was used to dissolve the compound. In the low-resolution mode, the peak at 805.0 *m/z*, due to the sodium salt form of TSUPQD, can be clearly identified and was measured under nitrobenzyl alcohol (NBA) and NaBr matrix.

In a second run, trace amounts (750 ppg) of poly(propylene glycol) were added as a mass calibration standard for the high-resolution runs. The exact match of the experimentally determined mass with the predicted mass (Table S1) further proves the high purity of the product

3.5. Elemental Analysis. As summarized in Table S2, each elemental mass percentage is in good agreement with the theoretical data. The negligible difference found for C and H (0.086% and 0.82% respectively) might be explained by the pre-hydrolysis of the ethoxysilane-end group. Compared with freshly synthesized samples, the results after recrystallization are closer to the theoretically calculated values, probably because of higher purity of the samples. Therefore, we conclude that the empirical formula is close to the theoretical one, viz. $C_{38}H_{58}N_6O_8Si_2$, which is consistent with mass and ^{1}H NMR spectra results.

3.6. Thermal Study by Thermal Gravimetric Analysis (TGA) and Differential Scanning Calorimetry (DSC). We investigated the thermal stability of this novel electroactive silsesquioxane by heating samples up to 700 °C at a rate of 20 °C/min in air. The negligible weight loss below 100 °C is probably due to the residual moisture in the sample. As shown in Figure 3A, the major decomposition of purified TSUPQD occurs at ∼220−240 °C, with a secondary decomposition at ∼550 °C, which can be attributed to the thermal degradation of integrated propyl groups and conjugated aromatic groups, respectively. The weight loss curve of the freshly synthesized material shows a different profile with gradual decomposition from 270 to 600 °C. The remarkably different behavior of TSUPQD indicates that the novel compound is susceptible to

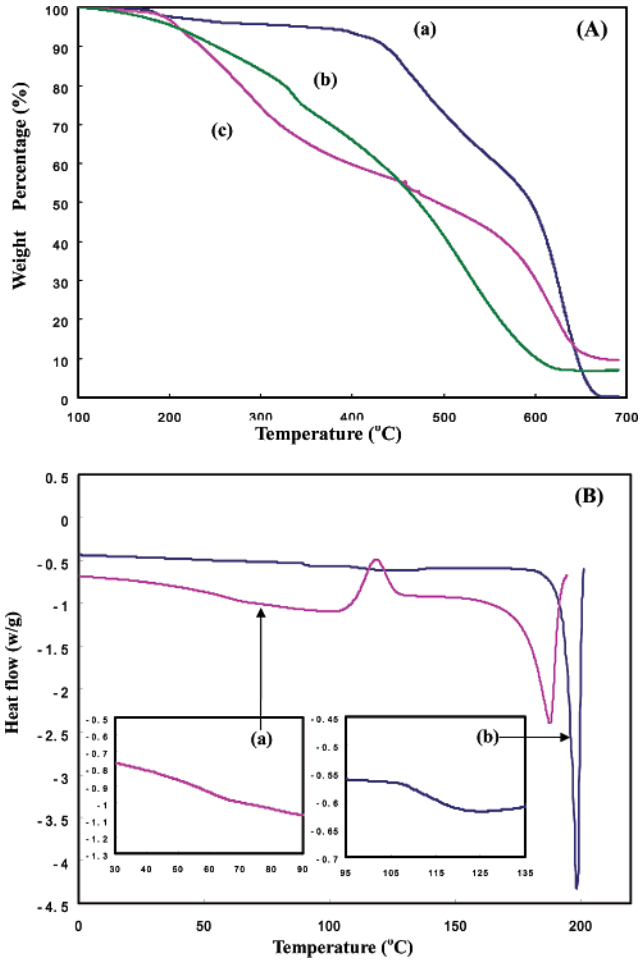

Figure 3. (A) TGA curves of (a) emeraldine-base aniline trimer, (b) recrystallized TSUPQD, and (c) freshly synthesized TSUPQD. (B) (a) DSC curve of freshly synthesized TSUPQD and (b) recrystallized TSUPQD. The inset shows the T_g of compounds from a magnified view.

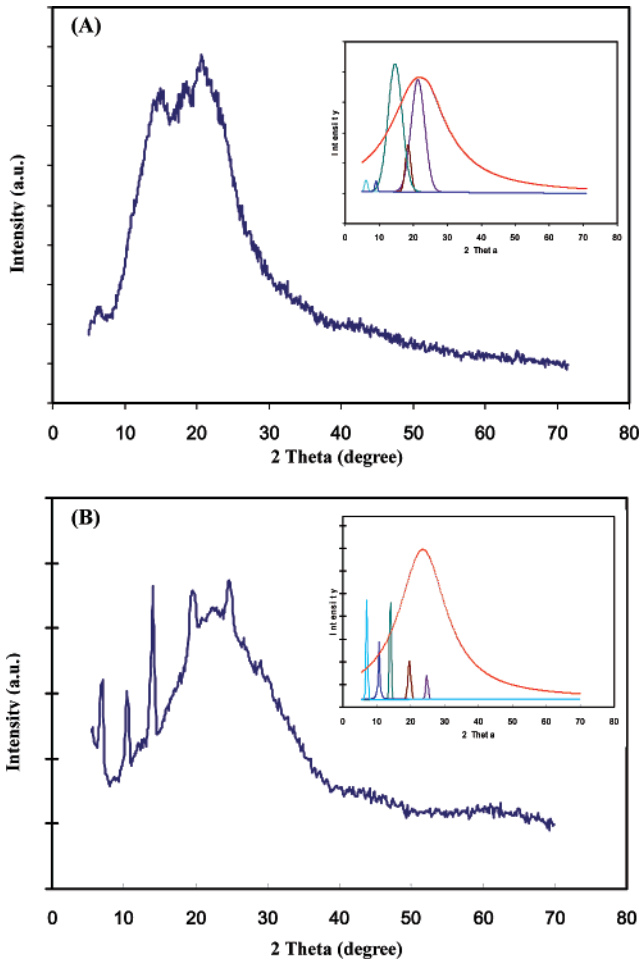

Figure 4. Separation of X-ray Debye−Scherrer pattern from TSUPQD for crystalline component, amorphous component and the baseline: (A) XRD of as-synthesized TSUPQD; (B) XRD of recrystallized TSUPQD

thermal treatment compared with the starting compound, aniline trimer, due to easier degradation from its triethoxylsilylpropyl moiety in the backbone. Another feature is the higher residual weight of TSUPQD due to the existence of SiO_2 moieties after annealing. When compounds are heated to 700 °C, at which temperature the residues can keep constant weight, recrystallized TSUPQD shows 9.6 wt % SiO_2 residue, whereas the aniline trimer undergoes complete thermal degradation.

To further assess the thermal behavior, such as the endothermic and exothermic process, of the novel product TSUPQD, differential scanning calorimetry study (DSC) was performed under air using TA Instruments Q100 with two temperature cycles varying from −50 to +200 °C at a 5 °C /min cooling rate and 10 °C/min heating rate (Figure 3B). The amount of each sample used in the sample cell was 3 mg. The result of DSC study clearly supports the notion that the crystalline domain has been altered during the recrystallization process. The differential heat flow curve for freshly synthesized TSUPQD in Figure 3B-a displays that one small endotherm appears at ca. 52 °C indicating the glass transition temperature (T_g) and one sharp endotherm, at ca. 188 °C attributed to the main phase transition temperature (T_m). In addition, the onset of the intensive exotherm peak at 130 °C further illustrate that some of TSUPQD molecules crystallized owing to enhanced intermolecular interaction (hydrogen bonding) in elevated temperature, revealing that freshly synthesized TSUPQD is only partially crystalline. Thus, recrystallized TSUPQD (Figure 3B-b), as expected, exhibits improved crystalline properties and rigidity as there is a pronounced and significant shift for T_g which increases to 111 °C while the recrystallization exotherm vanishes completely. Meanwhile, T_m shows a slight increase to 195 °C. Furthermore, the main phase transition endotherm becomes stronger in endothermic heat content as well as sharper and more symmetric in the shape, suggestive of higher thermal resistance to disordered liquid phase for their well-packed crystal structure.

3.7. Powder X-ray Diffraction Study. X-ray diffraction measurements were carried out in a Rigaku XRD horizontal goniometer and recorded using a 2° 2θ step from 5° to 70° for each scan. The X-ray diffraction pattern, indicative of the structural properties of the EB form of TSUPQD is shown in the inset of Figure 4. Through appropriate curve fitting, the amorphous domain can be approximated by a full Lorentzian while the crystalline regions are summarized as Gaussians. This procedure facilitates deducing the *d*-spacing from the angular position. The *d*-spacings, calculated according to Bragg's formula: $\lambda = 2d(\sin\theta)$, are tabulated in Table 1.

The XRD diffractions of freshly synthesized and recrystallized EB forms of TSUPQD (Figure 4, parts A, B), showed different patterns in terms of the low angle diffraction peaks. The recrystallized product displayed the sharper and more intense crystalline rings on top of a broad amorphous bump that demonstrates crystalline structure is only partially formed during synthesis. This statement is in good agreement with DSC analysis results. The optimized patterns of both TSUPQD, are mainly composed of one intense and broad ring centered at ca. $2\theta \sim 21°$ ($d \sim 2.25$ Å), which is featured as the amorphous

Table 1. *D*-Spacing, Intensity Corresponding to X-ray Experimental Pattern of TSUPQD[a]

TSUPQD as synthesized		TSUPQD as recrystallized	
d-spacing, Å	(*hkl*)	*d*-spacing, Å	(*hkl*)
14.73 s	(001)	12.49 l	(102)
9.83 s	(102)	8.28 l	(002)
6.03 l	(010)	6.29 l	(010)
4.80 m	(200)	4.51 m	(200)
4.13 l	(210)	3.58 m	(210)

[a] Abbreviation for intensity: s = small, m = middle and l = large.

domain, and five inner rings with a 2θ position ranging from ca. 6 to 25°, which are actually superimposed on the broad amorphous region. As stated above, because of their well-defined structure, aniline trimers have been used as computational models. As a derivative of polyaniline, TSUPQD should also show exhibit a similar crystalline structure with ordered benzenoid and quinoid sequences. From the structural point of view, two classes of EB form of polyaniline have been distinguished viz., EB-1 and EB-2.[28] The EB-1 form can further be divided into two patterns, EB-1α and EB-1β, differing in the position and shape of the low angle peaks: the presence of water molecules has been shown to influence the structural pattern of the EB form of polyaniline.[29] The samples in this study were pretreated with water prior to the XRD measurements. Indeed, the XRD data indicated that the crystalline region of the recrystallized TSUPQD resembled the calculated diffraction patterns of polyaniline EB-1β, with positions in 2θ at 8, 12, 15, 20, and 24, respectively, while freshly synthesized TSUPQD was similar to EB-1α model, with positions in 2θ at 6, 9, 15, 19, and 23, respectively. The relative intensity ratio of all these peaks is subject to the mode of water adsorption and is also sensitive to the water molecule arrangement. When doped with HCl, TSUPQD turns into the ES type, however, with a less degree of crystallinity (Figure S3). This observation is different from what is known for HCl-doped ES types of polyaniline[28] and may be caused by an impairment of intermolecular hydrogen bonding, the interaction that contributes to the higher crystalline order in TSUPQD.

3.8. Cyclic Voltammograms. The cyclic voltammogram of TSUPQD was recorded in an aqueous solution of HCl (Figure 5). Since the analyte is insoluble in aqueous solutions, a film was deposited on the electrode by casting a solution of TSUPQD in ethanol (5 mg/mL) on top of the working electrode and drying it in air. The cyclic voltammograms were expected to be essentially similar to the voltammograms of the HCl-doped ES form of polyaniline[30] except that the second redox pairs were absent in the scanned range of potentials due to background limit from water. In this potential range a pair of well-defined redox peaks at around 500 mV represent the removal/addition of 2 electrons (Figure 5A) and can be attributed to the reversible redox process from the "leucoemeraldine" to the ''emeraldine" forms.

The electrochemical behavior of TSUPQD was further examined in nonaqueous solutions. As before, in the aqueous solution, a pair of redox peaks was observed for TSUPQD in the lower potential range. Without the high background of water, we noticed a second pair of peaks corresponding to the oxidation of the "emeraldine" form to the "pernigraniline" form with a formal potential at 985 mV (Figure 5B), which is slightly higher than that of polyaniline. This is reasonable and may be attributed to the electron withdrawing ureido group of TSUPQD.

3.9. Optical Microscopy of HCl-Doped TSUPQD. Figure 6 shows microscopic images (transmitted light, 1000× objective) of HCl-doped TSUPQD obtained with an Olympus PMG-3

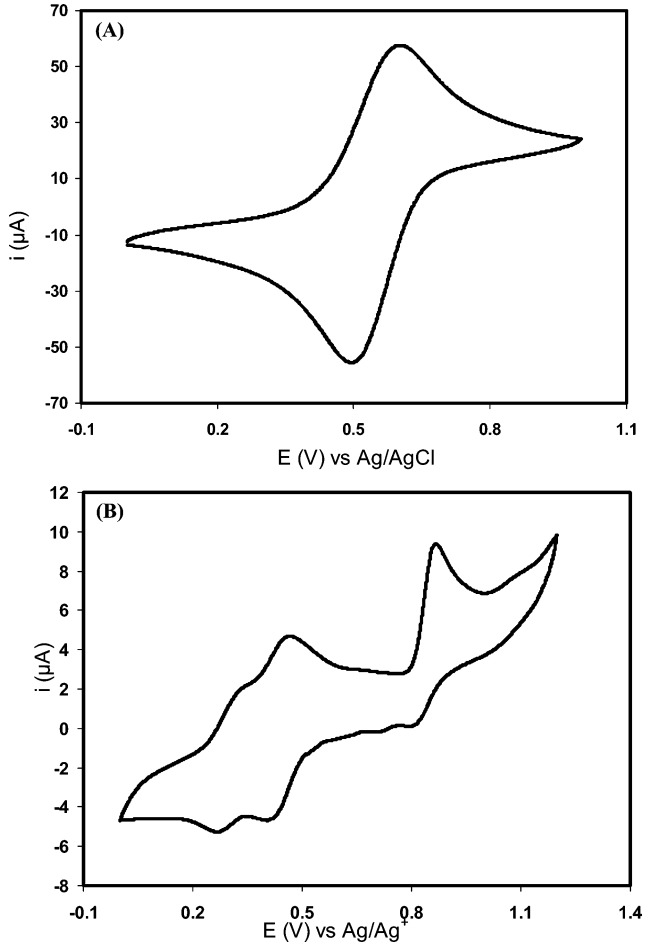

Figure 5. (A) Cyclic voltammogram of TSUPQD in aqueous solution of HCl (1 M). A trimer-film electrode was prepared by casting the trimer solution in ethanol (5 mg/mL) on top of the working electrode and then drying it in air. The scan rate used was 60 mV/s. (B) Cyclic voltammogram of TSUPQD in acetonitrile containing 0.1 M Et_4NPF_6 and 0.77 M $MeHSO_4$.

optical microscope. The continuously enhanced intermolecular interaction suggests an evolution from insulating single EB crystals to form electroactive aggregates. Without doping with HCl, TSUPQD is in the form of individual particles (Figure 6A), but when protonated with acid, the product apparently aggregates into complexes consisting of radical cations via proton−electron transfer. In this way, the TSUPQD molecules are prone to formation of intermolecular networks due to the acid-catalyzed condensation and behaving like polyaniline to delocalize the electrons through the closely packed macromolecular chains. With increasing degree of doping (Figure 6B−D) the doped products can optimize intermolecular interactions and conductivities to form a unique network at a doping ratio as high as 1:500. These results are in agreement with the electronic spectra acquired above.

As seen in the synthesis pathway depicted in Scheme 1, this preparation is solely based on the isocyanato-amine coupling reaction without using any catalyst and any byproduct. Thus, the purity of as-synthesized compound can be simply controlled by the equal molar addition of reactants, as easily monitored by ^{1}H NMR, mass spectra and elemental analysis. The whole process of synthesis is to be carried out under N_2 protection to prevent the ethoxysilane units from hydrolysis and condensation. Furthermore, after several crystallization steps, the purity of the product can be further increased though the yield and purity of the freshly prepared product was remarkably high. This process

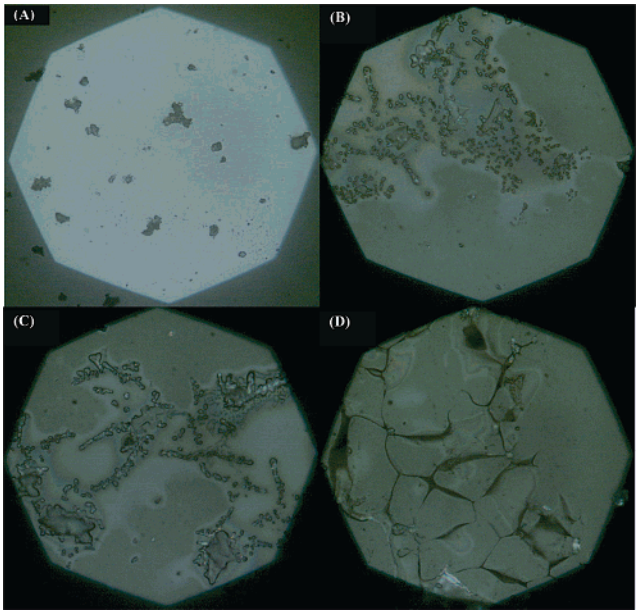

Figure 6. Optical microscopy images (transmitted light, 1000 × objective) of HCl-doped TSUPQD films prepared by dip-coating method: (A) Undoped TSUPQD; (B) 1:10 HCl-doped TSUPQD; (C) 1:80 HCl-doped TSUPQD; (D) 1:500 HCl-doped TSUPQD.

has been evidenced by the DSC analysis and XRD measurement. The nonredox doping of this novel compound TSUPQD with protonic acids can yield the conductive emeraldine salt state and the charges can delocalize within the backbone as depicted in Scheme 2. This reversible process has been investigated by detailed UV−vis spectra and electrochemical study, indicating the retention of its intrinsic electroactivity because they illustrated the results similar to those of polyaniline. On the basis of the above characteristics, it can be suggested that other aniline oligomers or amine-capped compounds could also be covalently integrated into silica frameworks by using the similar approach exploited here. The physiochemical properties of novel aniline trimer-contained hybrid siliceous materials were also explored in the following section for making electroactive PMOs for more applications.

Section B. Electroactive Polymeric Hybrid Material through Sol—Gel Process. A novel electroactive hybrid material was obtained through the sol−gel reactions of TSUPQD with TEOS at various compositions. When more organic units are incorporated into the silica matrix, the polymeric material will became darker in color and thermally less stable. To exclude the possibility of simple physical entrapment or mere surface attachment, all samples were washed and sonicated with ethanol repeatedly before characterization.

3.10. Infrared Spectra of Hybrid Materials. The molecular structure of the resulting electroactive hybrid materials from TSUPQD and TEOS co-condensation was confirmed by the FT−IR spectra shown in Figure 7. The spectra have band patterns analogous to the TSUPQD model compound reported previously with slight changes upon the loading of TSUPQD. For instance, the broad band in the region of 3400−3600 cm^{-1} (Figure 7e) assigned to O−H stretching vibration from TEOS will gradually move to 3300 cm^{-1} (Figure 7a) that is associated with N−H stretching vibration with increasing amount of TSUPQD. On the other hand, it is not surprising to find that all characteristic peaks from TSUPQD will be increasingly attenuated in pure silica from TEOS as the amount of organic bridge decreases. Some of those characteristic peaks include the peak at ca. 2900 cm^{-1} for aliphatic groups, 1670 cm^{-1} for carbonyl

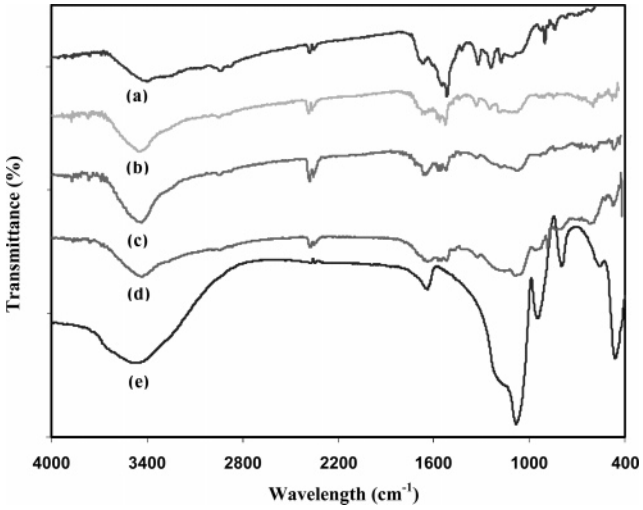

Figure 7. FTIR spectra for series of TSUPQD-TEOS hybrid material through sol−gel process: (a) 100 wt % electroactive organosilica from TSUPQD, (b) 50 wt % organosilica from TSUPQD-TEOS, (c) 25 wt % organosilica from TSUPQD-TEOS, (d) 10 wt % organosilica from TSUPQD-TEOS, and (e) pure silica from TEOS as control.

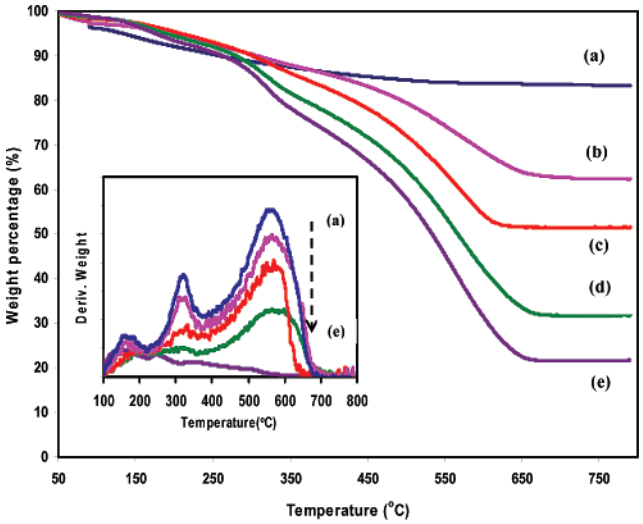

Figure 8. TGA of hybrid material from TSUPQD-TEOS at different weight percentage of TSUPQD: (a) 0 wt %, (b) 10 wt %, (c) 25 wt %, (d) 50 wt %, and (e) 100 wt %. Inset: TGA differential curves with plot of derivative weight percentage against temperature.

groups, 1512 and 1586 cm^{-1} for benzene rings and quionone stretching mode, 1316 cm^{-1} for C−N stretching vibration arising from aromatic amine groups and 1168 cm^{-1} for N = Q = N (Q is quinoid group) stretching vibration.[27]

3.11. Thermal Study of Hybrid Materials by TGA. TGA measurements were carried out on all samples. As seen in Figure 8, the thermal stability of the materials increased with the silica content. At temperatures as high as 750 °C, all organic content was decomposed and only white solid SiO_2 remained. The samples prepared in the absence of TSUPQD or at low concentrations of TSUPQD (e.g., below 25 wt % sol B) showed considerable thermal resistance losing <50% in weight. However, as more organic bridges were integrated into silica frameworks, the less stable the resulting samples became. A differential TGA curves with the derivative weight percentage against temperature suggests that there are three main decomposition stages for each sample (Figure 8 insert). The early stage of decomposition for hybrid materials (at 160−180 °C) is associated with loss of ethylortho groups followed by a rapid degradation of aromatic chains at 320 and 600 °C. That could

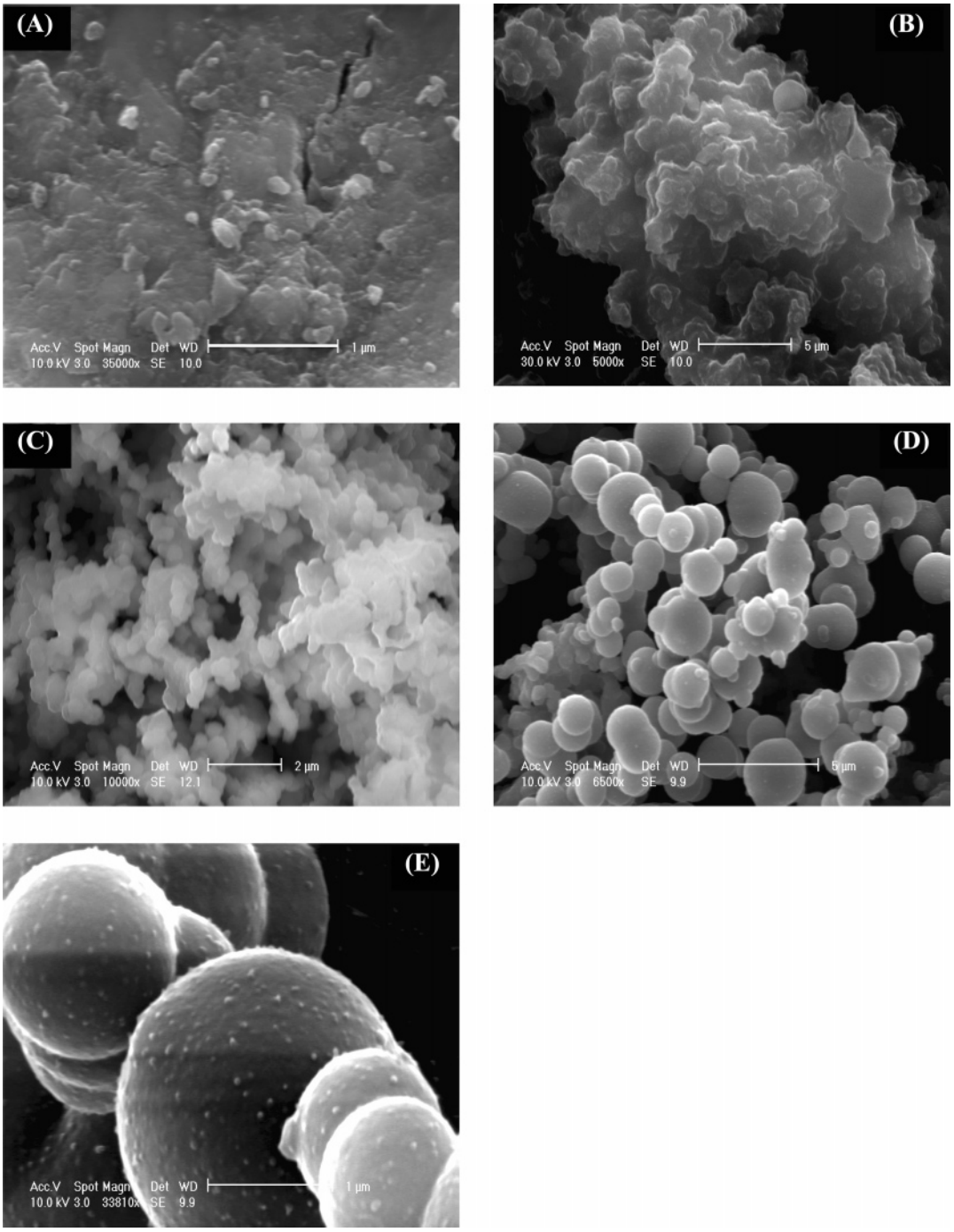

Figure 9. SEM images of as-synthesized hybrid materials from TSUPQD-TEOS at different weight percentage of TSUPQD: (A) 0 wt %; (B) 25 wt %; (C) 50 wt %; (D) 100 wt %; (E) magnified view of 100 wt %.

be visually validated by the fact that only white solid SiO_2 remained after heating without any black organic residue. Moreover, the amount of the remaining silica agreed with the initial sample composition. For example, in the case of 100 wt % TSUPQD siliceous hybrid material, the sample yielded 21.7% SiO_2 at 800 °C, which is reasonably consistent with the theoretical value of 20.9% SiO_2 in the sample composition.

3.12. Ultrastructural Study by Scanning Electron Microscopy (SEM). The ultrastucture of freshly synthesized hybrid materials prepared under the same environmental condition for sol−gel reactions was studied by SEM. (Figure 9) The shape of the new materials depended to a large extent on the content of organic bridges integrated. When the silica was made from pure TEOS (Figure 9a), a completely amorphous phase was observed. As the TSUPQD contents were increased from 25 to 100 wt %, the morphology of the hybrid material changed into solid microspheres. This transition suggests that with an increase of the organic content the initially rough and ridged surface of TEOS-made silica gradually turns into highly ordered organosilica, due to the tendency of tight packing driven by the intermolecular hydrogen bonding from TSUPQD. The size of solid spheres is narrowly distributed, ranging from 1 to 2.5 μm. The conductivity of spherical organosilica was 1.3×10^{-4} S/cm, a remarkable improvement after condensation polymerization.

4. Conclusion

A novel electroactive silsesquioxane precursor, *N*,*N*′-bis-(4′-(3-triethoxysilylpropylureido)phenyl)-1,4-quinonene-

diimine (TSUPQD), has been successfully synthesized and extensively characterized. The preparation of this ethoxysilane-capped compound was achieved via a one-step coupling reaction between amine-capped aniline trimer and triethoxysilylpropyl isocyanante. The molecular structure of TSUPQD was confirmed by FT−IR, NMR, mass spectra, and elemental analysis; its unique electroactive property was studied by UV−vis spectroscopy and cyclic voltammetry. With such a well-defined structure and reversible electrochemical properties, TSUPQD can be useful in developing new substrate materials for diverse applications, such as electrospun nanofibrous scaffolds in tissue engineering and modified electrodes for electrocatalysis. The approach exploited in this paper can also be used to covalently distribute other aniline oligomers or amine-capped compounds into silica frameworks to explore a broad range of new organic−inorganic hybrid materials. Upon co-condensation of TSUPQD and TEOS, prehydrolyzed TSUPQD mixes homogenously with TEOS sols to yield spherical organosilica particles in the presence of cosolvent ethanol. The intrinsic properties of the resulting hybrid materials are largely dependent on the loading of organic bridges.

Acknowledgment. This work was supported in part by the US Army Research Office (ARO), National Institutes of Health (NIH No. DE09848), and the Commonwealth of Pennsylvania through a grant to the Nanotechnology Institute of Southeastern Pennsylvania.

Supporting Information Available: Figures showing ^{1}H, ^{13}C, and ^{29}Si NMR spectra,for TSUPQD, mass spectrum of TSUPQD, and XRD spectra of TSUPQD and tables of experimental and calculated mass specteal data and elemental analyses for TSUPQD. This material is available free of charge via the Internet at http://pubs.acs.org.

References and Notes

(1) Kresge, C. T.; Leonowicz, M. E.; Roth, W. J.; Vartuli, J. C.; Beck, J. S. *Nature (London)* **1992**, *359*, 710.
(2) Hench, L. L.; Araujo, F. G.; West, J. K.; La Torre, G. P. *J. Sol-Gel Sci. Technol.* **1994**, *2*, 647.
(3) Kuraoka, K.; Kakitani, T.; Suetsugu, T.; Yazawa, T. *Sep. Purif. Technol.* **2001**, *25*, 161.
(4) Kuenzelmann, U.; Boettcher, H. *Sens. Actuators, B* **1997**, *B39*, 222.
(5) Wei, Y. *Encycl. Mater. Sci. Technol.* **2001**, 7594.
(6) Asefa, T.; MacLachlan, M. J.; Coombs, N.; Ozin, G. A. *Nature (London)* **1999**, *402*, 867.
(7) Inagaki, S.; Guan, S.; Fukushima, Y.; Ohsuna, T.; Terasaki, O. *J. Am. Chem. Soc.* **1999**, *121*, 9611.
(8) Hunks, W. J.; Ozin, G. A. *J. Mater. Chem.* **2005**, *15*, 3716.
(9) Burleigh, M. C.; Markowitz, M. A.; Jayasundera, S.; Spector, M. S.; Thomas, C. W.; Gaber, B. P. *J. Phys. Chem. B* **2003**, *107*, 12628.
(10) (a) Che, S.; Liu, Z.; Ohsuna, T.; Sakamoto, K.; Terasaki, O.; Tatsumi, T. *Nature (London)* **2004**, *429*, 281. (b) Asefa, T.; MacLachlan, M. J.; Grondey, H.; Coombs, N.; Ozin, G. A. *Angew. Chem., Int. Ed.* **2000**, *39*, 1808. (c) Sayari, A.; Hamoudi, S. *Chem. Mater.* **2001**, *13*, 3151. (d) Inagaki, S.; Guan, S.; Ohsuna, T.; Terasaki, O. *Nature (London)* **2002**, *416*, 304. (e) Kapoor, M. P.; Yang, Q.; Inagaki, S. *J. Am. Chem. Soc.* **2002**, *124*, 15176. (f) Furukawa, H.; Hibino, M.; Zhou, H.; Honma, I. *Chem. Lett.* **2003**, *32*, 132.
(11) Alvaro, M.; Ferrer, B.; Garcia, H.; Rey, F. *Chem. Commun.* **2002**, *18*, 2012.
(12) Hunks, W. J.; Ozin, G. A. *Chem. Mater.* **2004**, *16*, 5465.
(13) (a) Skotheim, T. A.; Elsenbaumer, R. L. Reynolds, J. R. *Handbook of conducting polymers*, 2nd ed.; Marcel Dekker: New York, 1997. (b) Kovacic, P.; Timberlake, J. W. *Polym. J.* **1988**, *20*, 819. (c) Wessling, B. *Handb. Nanostruct. Mater. Nanotechnol.* **2000**, *5*, 501.
(14) Sein, L. T., Jr.; Wei, Y.; Jansen, S. A. *J. Phys. Chem. A* **2000**, *104*, 11371.
(15) Jansen, S. A.; Duong, T.; Major, A.; Wei, Y.; Sein, L. T., Jr. *Synth. Met.* **1999**, *105*, 107.
(16) Lu, F. L.; Wudl, F.; Nowak, M.; Heeger, A. J. *J. Am. Chem. Soc.* **1986**, *108*, 8311.
(17) MacDiarmid, A. G.; Zhou, Y.; Feng, J. *Synth. Met.* **1999**, *100*, 131.
(18) Sein, L. T., Jr.; Wei, Y.; Jansen, S. A. *Polym. Prepr.* **2000**, *41*, 1741.
(19) Sein, L. T., Jr.; Wei, Y.; Jansen, S. A. *Synth. Met.* **2000**, *108*, 101.
(20) Wei, Y.; Yang, C.; Ding, T. *Tetrahedron Lett.* **1996**, *37*, 731.
(21) Feng, Q.; Xu, J.; Dong, H.; Li, S.; Wei, Y. *J. Mater. Chem.* **2000**, *10*, 2490.
(22) Wei, Y.; Feng, Q.; Xu, J.; Dong, H.; Qiu, K.; Jansen, S. A.; Yin, R.; Ong, K. K. *Adv. Mater.* **2000**, *12*, 1448.
(23) (a) Guterman, E.; Cheng, S.; Palouian, K.; Bidez, P.; Lelkes, P. I.; Wei, Y. *Polym. Prepr.* **2002**, *43*, 766. (b) Guo, Y.; Wei, Y.; Lelkes, P. I.; Ko, F.; Zhou, Y.; Levon, K. *Polym. Mater. Sci. Eng. Prepr.* **2004**, *91*, 585.
(24) Li, M.; Guo, Y.; Wei, Y.; MacDiarmid, A. G.; Lelkes, P. I. *Biomaterials* **2006**, *27*, 2705.
(25) Wan, M. *J. Polym. Sci., Part A: Polym. Chem.* **1992**, *30*, 543.
(26) Lokshin, N. A.; Pyshkina, O. A.; Golubev, V. B.; Sergeyev, V. G.; Zezin, A. B.; Kabanov, V. A.; Levon, K.; Piankijsakul, S. *Macromolecules* **2001**, *34*, 5480.
(27) (a) Quillard, S.; Louarn, G.; Lefrant, S.; Masters, J.; MacDiarmid, A. G. *Phys. Rev. B.: Condens. Matter* **1994**, *50*, 12498. (b) Harada, I.; Furukawa, Y.; Ueda, F. *Synth. Met.* **1989**, *29*, E303. (c) Furukawa, Y.; Ueda, F.; Hyodo, Y.; Harada, I.; Nakajima, T.; Kawagoe, T. *Macromolecules* **1988**, *21*, 1297.
(28) (a) Pouget, J. P.; Jozefowicz, M. E.; Epstein, A. J.; Tang, X.; MacDiarmid, A. G. *Macromolecules* **1991**, *24*, 779. (b) Laridjani, M.; Pouget, J. P.; Scherr, E. M.; MacDiarmid, A. G.; Jozefowicz, A. J.; Epstein, A. J. *Macromolecules* **1992**, *25*, 4106. (c) Winokur, M. J.; Mattes, B. R. *Macromolecules* **1998**, *31*, 8183.
(29) Luzny, W.; Sniechowski, M.; Laska, J. *Synth. Met.* **2002**, *126*, 27.
(30) (a) Focke, W.; Wnek, G. E. *J. Electroanal. Chem. Interfacial Electrochem.* **1988**, *256*, 343. (b) Genies, E. M.; Tsintavis, C. *J. Electroanal. Chem. Interfacial Electrochem.* **1985**, *195*, 109.

MA0622985